Dielectric constant and conductivity anisotropy measurements of Schiff base liquid crystal

Dielectric constant and conductivity anisotropy measurements of Schiff base liquid crystal

Hussain A. Badran[1] , Harith A. Hasan[1,2]

[1]Department of Physics,College of Education for Pure science, University of Basrah, Basrah,Iraq
[2]Department of Material Science, Polymer Research Centre, University of Basrah, Basrah, Iraq
[1]hussain_badran @yahoo.com
[2]Corresponding author: harth.alqata100@yahoo.com

Abstract. The liquid crystal (LC) compound with the central linkage group Schiff-base was studied. The molecular structure was characterized with FTIR. Mesomorphic properties were characterized using differential scanning calamity (DSC) and polarizing optical microscopy (POM). The dielectric constant (ε) with conductivity (σ) and dielectric anisotropy (Δε) have been measured in the frequency range of 100 Hz to 100 MHz from room temperature to 100 °C. Dielectric constants parallel and perpendicular to helical axes (ε_{II} and $\varepsilon_{\perp}$), the dielectric anisotropy ($\Delta\varepsilon = \varepsilon_{II} - \varepsilon_{\perp}$) and conductivity (Δσ) have been determined in different mesophases. Activation energy (E_{ac}) of the a.c. conduction process and threshold voltage (V_{th}) of the sample sandwiched in the liquid crystal cell have been determined in different mesophases. The electro-optic effect was also studied at liquid crystal phase temperatures. The Schiff-base liquid crystal sample exhibiting a nematic phase.

Keyword: liquid crystal; dielectric anisotropy; activation energy; threshold voltage; Nematic threads.

INTRODUCTION

Schiff bases are organic compounds containing the isomethine group (methinc group - CH =) [1-3]. It was first brought up by the German scientist Hugo Schiff in 1864 by condensing aldehydes or aliphatic or aromatic ketones with elementary amines (aliphatic or aromatic) hence the name (Aldimine). When it is derived from aldehyde through condensation between the carbonyl group and the primary amines, as the monoalkyl amine (R-NH_2) or the monoeryl amine (Ar-NH_2) is added to the carbon of the carbonyl group of aldehyde or ketone and the intermediate compound Carbinolamine is formed, followed by Loss of a water molecule to form N-substituted imine, which represents Schiff's base as the final product [4,5]. Organic compounds and Schiff's basic liquid crystals have been almost prominent in many applications, such as, in the paper industry, solar applications[6],food dyes[7],Biological applications[8,9],conducting polymer [10], Biopolymer applications[11], nano-particle applications[12,13], nano-composed[14,15], photovoltaic applications[16],NMR application [17], data storage [18], dosimeter applications[19-21], nonlinear applications [22], all-optical switching [23], thermal lens applications[24,25], optical limiting [26-28], limiter device[29,30] and liquid crystal displays. Some azomethine compounds are very attractive materials due to rich liquid crystalline polymorphism [31]. The state of the liquid crystals was between the conventional solid and liquid phases, and that's where the term “mesogenic state” came from. Liquid crystalline materials have numerous applications in scientific and technological fields, in organic light-emitting diodes [32-34], photoconductors [35], anisotropic arrays and semiconductor materials [36]. The strong demand for new liquid crystals for applications has led to the synthesis and study of numerous mesogens especially, thermotropic liquid crystals [37-39]. Most thermotropic liquid crystals are stem-shaped molecules with a rigid core

with one or more phenyl rings and one or more flexible end-alkyl groups [40,41]. Extensive studies of Schiff base systems have been conducted since the discovery of N- (4-Methoxy benzylidene)-4-butylaniline (NBBA) with an ambient temperature nematic phase[42]. Several studies have been performed on the basic esters of Schiff because of their interesting properties and their substantial temperature range [43-46]. Typical endpoints demonstrated that the properties of liquid crystals are those of the azomethine group. Polar placers have strong dipolar moments, they can promote mesomorphic properties. In this paper, we report the temperature and frequency dependence of the dielectric constant (ε) with conductivity (σ), dielectric anisotropy (Δε) and the activation energy of liquid crystal mixtures of N- (4-Eethoxy benzylidene)-4-butylaniline. The Schiff base LC exhibits a nematic A phase.

EXPERIMENTAL METHODS

GENERAL FORMULAE AND FT-IR ANALYSIS

We have been prepared liquid crystal belonging to Schiff base compound whose general chemical formulae is shown in Figure1.

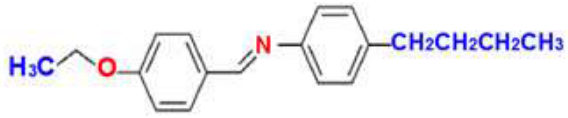

FIGURE 1. general formulae of LC compound

FT-IR Spectrometer model Perkin-Elmer System 2000 has been using to recorded IR spectra of a Schiff base LC compound. The stretching vibration of the functional groups of N- (4-Eethoxy benzylidene)-4-butylaniline Schiff base LC was shown in Fig.2, which confirmed that the method of alkylation for para hydroxyl benzaldehyde is correct. Figure 2 shows the measured Fourier Transform Infrared spectrum of the synthesized organic compound in the range (4000–400) cm^{-1}. It can be seen from the figure the IR that, two strong peaks of aromatic double bond C=C stretching emerged at 1604-1569 cm^{-1}. The bands in this region have contribution mainly from C=N (1250.61) cm^{-1}, C-N(1162.07 cm^{-1},C-O(1465.63) cm^{-1} stretch, and C-H(3027.69) cm^{-1} aromatic bonds, and C-H(822.491)cm^{-1} bending aromatic ,.The stretching vibration of the O-C group which appeared at1507.1 cm^{-1} aromatic cancels the absorption peak of the ($-NH_2$) group supposed to appear at the same region. The peaks appeared in the region of 2923.56 cm^{-1} for the (CH_3) bond corresponding to the plane bending vibration of the aromatic C–H bond. The weak band at 2852.2 represents the asymmetrical (CH_2) and symmetrical stretching of the aliphatic C–H bond respectively.

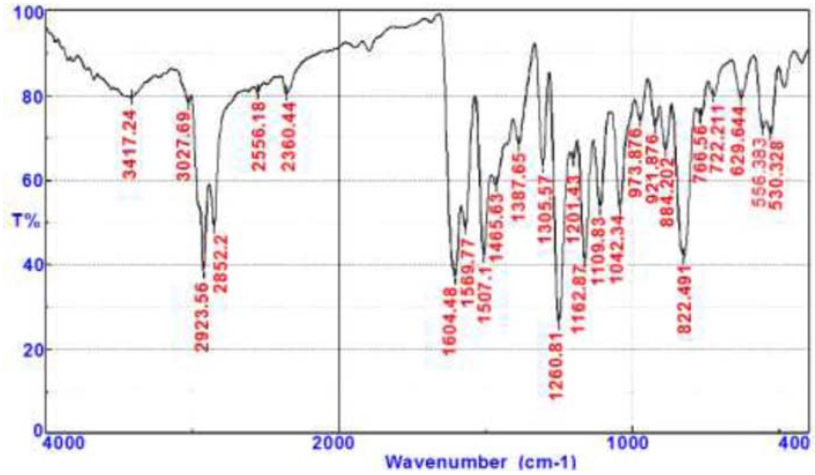

FIGURE 2. Infrared spectrum for NBBA Schiff base LC

SURFACE PREPARED OF ITO

SCHIFF BASE CELL PREPARATION

Because of its transparency, perfect conductivity, high hardness, hatchability and easy adherence on different types of substrates, indium tin oxide (ITO) is usually used as an electrode material. Glass slides coated with Commercially Indium Tin Oxide films (Baltracon-Balzers) with a thickness about 140 nm on glass substrates were used in the preparation of the electro-optical cell, which is easy to cut and flat enough to allow the manufacture of a cell with parallel surfaces, and since the used glass is conductive glass due to the presence of conductive coating material. Available ITO films (Baltracon-Balzers) with a thickness of around 140 nm on glass substrates. The surfaces of indium tin oxide substrates were treatment and cleaned according to the following method: 35 min in an ultrasonic bath of methanol followed by 25 min under acetone reflux in a soxhlet before being dried. This method was picking after an ordinal study of the effects of the ITO surface treatments on the performance of LCDs. The cellular assembly method consists of pouring the selected sample N- (4-Ethoxy benzylidene)-4-butylaniline) onto one of the processed glass electrodes, after which it heats for some time (ideally 10 to 15 minutes) above the clarity of the model to allow all of the trapped air to escape. After this process, the second glass electrode is installed over the first electrode and then the whole group is inserted into the Home Made Rapid" epoxy resin.

RESULTS AND DISCUSSION

OPTICAL MICROSCOPIC AND THERMAL BEHAVIOR STUDIES

Figure 3 shows the image captured by the polarized light microscope, as it shows the optical textures of the liquid crystal compound that was diagnosed during the heating process, moving from the solid crystal phase to the liquid crystal phase within the thermal range of the nematic phase 42.26 – 79.87 ^{o}C.

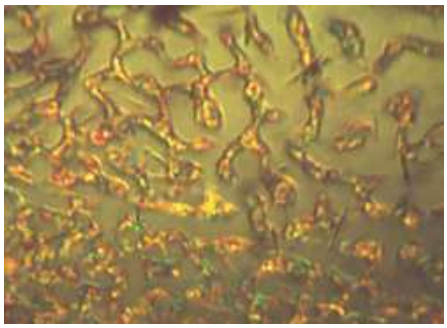

Figure 3. Nematic threads of NBBA LC

The phase transition of the NBBA Schiff base LC was identified by making use of a DSC thermo-gram for the experimental sample. The thermo-gram shows an efficient transition from crystal to nematic crystal phase with a transition temperature range of about 42 ^{o}C with an enthalpy(ΔH) of 439.05 jg^{-1} as shown in Fig.4. The thermal analyses by DSC thermo-gram for liquid crystal sample provide temperature range for L.C compound equal to 150 ^{0}C , the temperature range for anisotropic liquid crystal phase is 42.26 to 79.87, i.e. about 37.61 ^{o}C and melting point (T_m) is 33.4 ^{0}C.

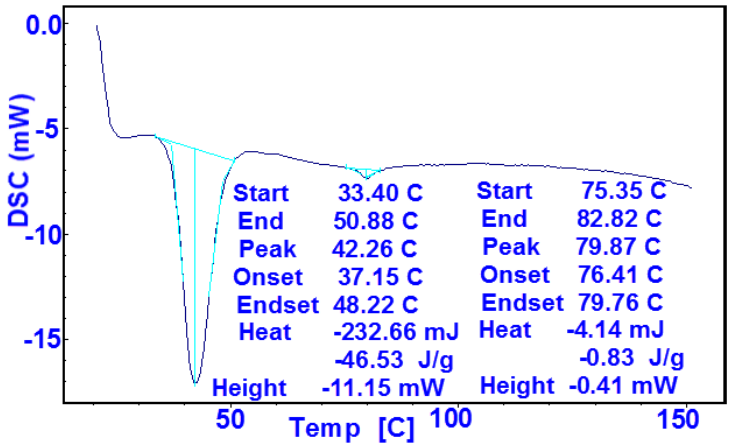

Figure 4. Thermal behavior of NBBA Schiff base liquid crystal during heating

The thermal analysis of the liquid crystalline compound using the DSC device gave the quantities of Enthalpy when moving from one phase to another and from that change in the enthalpy or the so-called latent heat associated with the phase transition, as well as determining the amount of energy absorbed or released heat flux, when the summit direction is down, the change is accompanied by the release of energy, and the direction of the summit to the top is accompanied by energy absorption. Table 2 shows these values for liquid crystalline compounds.

TABLE 1. Shows the thermal data for the liquid crystal compound.

Sold to L.C transition			L.C to Iso transition		
Enthalpy H(mj)	Latent heat ΔH(j/g)	Heat flux HF(mw)	Enthalpy H(mj)	Latent heat ΔH(j/g)	Heat flux HF(mw)
681.51	85.19	5.52	45.06	5.63	1.36

The composite showed a dielectric discrepancy($\Delta\varepsilon$) of 2.2, where the dielectric (ε) was measured without styling the molecules of the compound sample with a rise in temperature by heating through the liquid crystal phase (nematic), as well as measuring the dielectric with the styling of the longitudinal axes of the crystalline complex molecules by treating the conductive surface of the two slides. The ITO, by using some polymeric materials, casting in the form of a thin film, and then physically treating by rubbing in a fast and constant direction, we obtain two classes of parallel and perpendicular laying of the liquid crystalline particles.

The dielectric permittivity determines the response of the material to the external field. For anisotropic materials dielectric constant is a tensor (depends on the direction in space) ε_{II} component parallel to the optical axis and $\varepsilon_{\perp}$ component perpendicular to the optical axis). The dielectric anisotropy $\Delta\varepsilon = (\varepsilon_{II} - \varepsilon_{\perp})$ to the component well is positive because $\varepsilon_{II} > \varepsilon_{\perp}$. Fig. 6 shown dielectric constant as a function to the temperature for prepared samples during heating to the liquid crystal phase without any alignment.

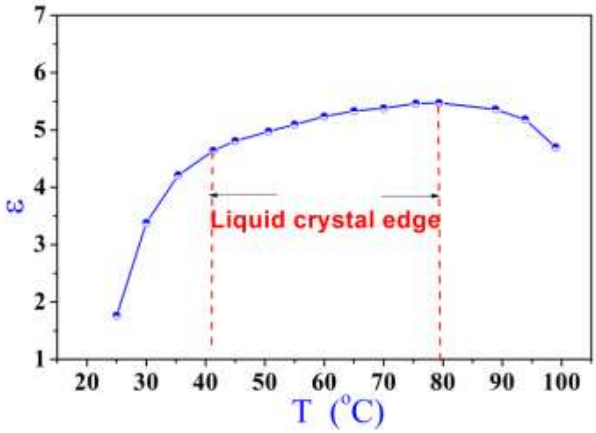

FIGURE 5 . The insulation changes (without styling) as the compound sample is heated

The electrical insulation has been measured ε_{II} in the case of parallel laying and electrical insulation $\varepsilon_{\perp}$ in the case of vertical layering with finding the contrast in the dielectric ($\Delta\varepsilon$) in the case of heating the nematic crystal compound sample through the liquid crystal phase.

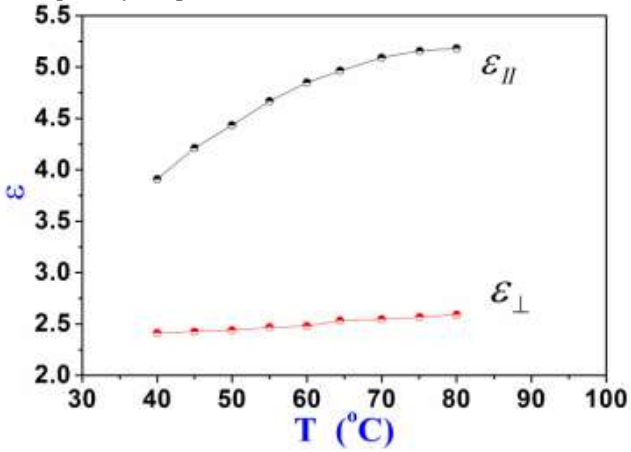

FIGURE 6. Parallel and vertical electrical insulation with partial longitudinal axis

Fig.7 shows the divergence between two insulation components during the liquid crystal phase. Figure 8 shows the behavior of the variation in the insulation ε during heating through the thermal range of the nematic crystal phase as well as the temperature of the transition to the isotropic phase are listed in Table 3.

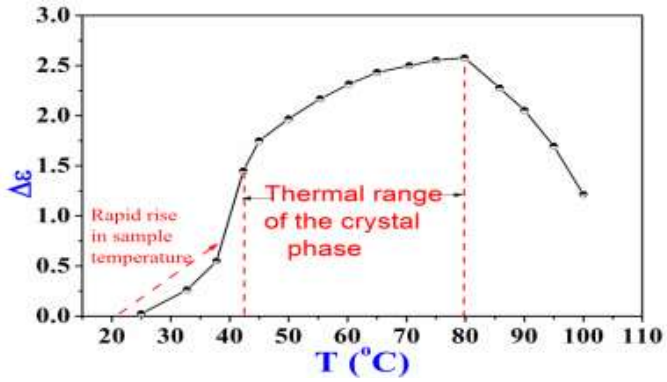

FIGURE 7. The variation in insulation changes with increasing temperature.

TABLE 2. The thermal range of the nematic phase and the transition temperature to the isotropic phase

L.C Temperature range ΔT (C°)	Melting point T_m (C°)	Phase transition temperature (C°)	
		L.C	Isotropic
37.61	33.4	42.26	79.87

CONDUCTIVITY MEASUREMENT

The conductivity measurement has been done both in perpendicular and parallel directions. The values of capacitance and dissipation factor of the cell holder with and without sample were determined. The electrical conductivity of liquid crystals is obeying the following equation [47]:

$$\sigma(\omega)_{ac} = \omega\varepsilon_{\circ}\varepsilon' \quad \text{……..(1)}$$

In which this equation represents a frequency dependent conductivity [48]:

$$\sigma(\omega)_{ac} = \frac{d}{AR_P} \quad \text{and} \quad R_P = \frac{1}{D\omega C_P} \quad \text{……..(2)}$$

Where d is the liquid crystal cell thickness, A is the cell cross-section area, R_P is the equivalent series resistance of the circuit, D is the dissipation factor, C_P is the equivalent parallel capacitance of the cell and ω is the angular frequency, the measured values of conductivity for our samples in both parallel and perpendicular alignments are given in figure 9 as well as The variation of conductivity anisotropy (σ) with temperature are given in figure 10 **.**

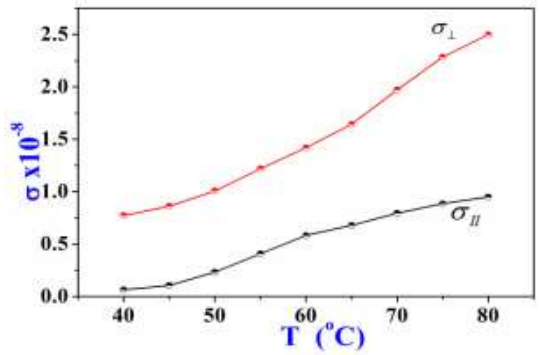

FIGURE. 8. Types of conductivity as a function of temperature

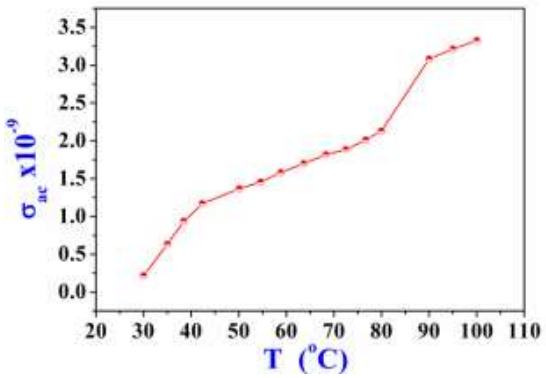

FIGURE. 9. Conductivity behavior as a function of temperature.

The cause of conductivity in liquid crystals bulk of L.C is either due to external (extrinsic) such as environment or due to the material itself i.e. intrinsic, or both due to ionic impurity and for this reason, the liquid crystal is semi-conducting and the conductivity is written according to Arinius relationship as follows [49,50]:

$$\sigma = \sigma_{\circ} \exp\left[-\frac{E_{ac}}{K_B T}\right] \qquad \text{……..(3)}$$

Where $\sigma_{\circ}$ is the ideal conductivity and is guessed at the area bounded between the points of intersection on the y-axis (it represents the conductivity values taken with the temperature values as the x-axis). The conductivity depends on ionic mobility μ and ionic concentration N, as well as the ratio $\sigma_{\perp}/\sigma_{II}$ conductivity ratio, is equivalent to mobility ratio $\mu_{\perp}/\mu_{II}$ [51]:

$$\sigma = qN\mu$$

……..(4)

Figure 11 represents the graph between the natural logarithm of the conductivity on the Y-axis versus(1/ T) in Kelvin units for the liquid crystal in the two states of non-alignment and parallel and perpendicular alignment of liquid crystal particles, and where the activation energy E_{ac} can be extracted from the graph for each state. The activation energy values in the case of non-alignment and the cases of parallel and vertical alignment are 0,404 , 0.424 and 0.361 eV, respectively.

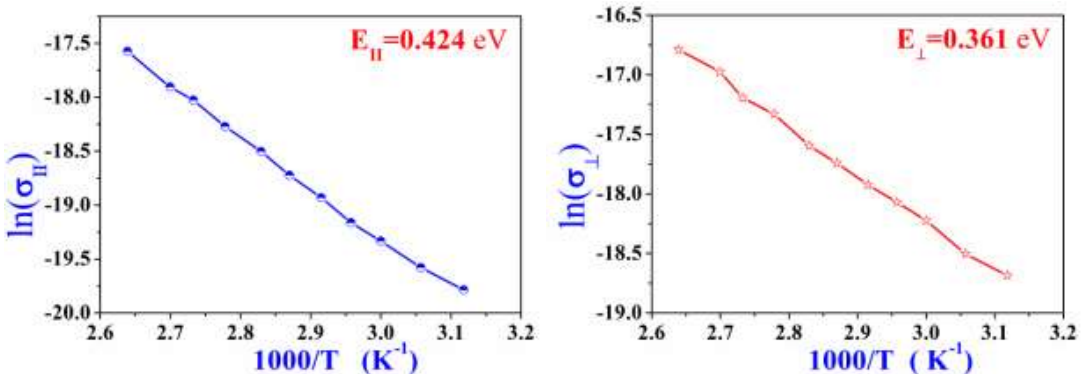

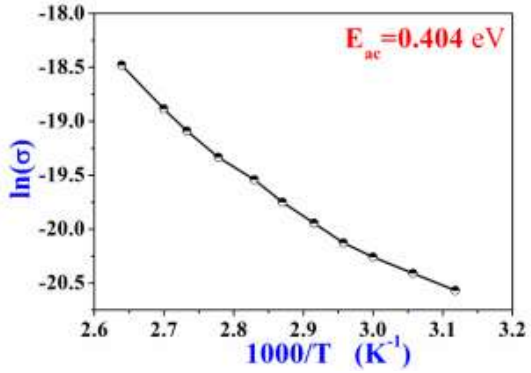

FIGURE 10. The Semi-logarithm of the conductivity Via. reciprocal of the temperature

CONCLUSION

In this paper, the central linkage group Schiff-base L.C molecular structure was characterized with FTIR. Mesomorphic properties were characterized using differential scanning calamity (DSC) and polarizing optical microscopy (POM). Also, we presented an investigation of the characteristics of the liquid crystal alignment layer and its effect on the electrical properties of the LC cell. We found that the high value of the dielectric permittivity at high temperature that's indicated to facts the molecular dipole will own high freely and movement with raising temperature degree to the nematic heating range as well as the dielectric anisotropy for the component was positive this indicated that's parallel dielectric component was higher than perpendicular component and this given explanation that molecular dipoles well be contributed higher at the parallel direction (parallel to the director) than perpendicular at liquid crystal temperature range and suggestive the angel between molecular dipole moment and longitudinal molecular axis approximately to $\beta \sim 0$ and this because of the presence of a high polarity terminal group.

REFERENCES

1. B. T. Thaker and J. B. Kanojiya, R. S. Tandel, Mol. Cryst. Liq. Cryst. **528**,120 (2010).
2. S. T. Ha, L. K.Ong, S. T. Ong, G. Y.Yeap, J. P.Wan Wong, T. M. Koh and H. C. Lin, Chinese Chemical Letters, **20**,767 (2009).
3. M. Sh. Hussain, Q. M. A. Hassan, H. A. Badran and C. A. Emshary, International Journal of Industrial Engineering & Technology (IJIET) **3**(4), 57 (2013).
4. K. Ichimura, Chem. Rev. **100**, 1847 (2000).
5. T. Ikeda, Journal of Materials Chemistry, **13**, 2037 (2003).
6. A. Al-Salihi, R. D. Salim, R. K. Fakher Alfahed and H. A.Badran, IOP Conf. Series: Materials Science and Engineering **928**,
072056 (2020).
7. H. A. Badran, A. Al-Maliki, R.K. Fakher Al-fahed, B.A. Saeed, A.Y. Al-Ahmad, F.A. Al- Saymari and R. S. Elias, J. of
Materials Science: Materials in Electronics **29**,10890 (2018).
8. N.A. Huda S.Yakop and H.A. Badran, Int. J. Eng. Res. Appl. **4**, 727 (2014).
9. N.A. Huda S.Yakop and H.A. Badran, International J. of Engineering Research And Management (IJERM) **1**, 67 (2014).
10. H.A. Badran, H.F. Hussain and K.I. Ajeel, Optik **127,** 5301(2016).

11. H.A. Badran, IOSR J. Appl. Phys. **1**, 33 (2012).
12. R.K. Fakher Alfahed, A.S. Al-Asadi, H. A. Badran and K.I.Ajeel, Applied Physics B,**125**, 48 (2019).
13. H.A. Badran, K.I. Ajeel and H.G. Lazim, Materials Research Bulletine **76**, 422 (2016).
14. H.G. Lazim, K. I. Ajeel and H. A. Badran, Spectrochim. Acta Part A Mol. Biomol. Spectrosc. **145**, 598 (2015).
15. H. A. Al-Hazam, R. K.Fakher Alfahed, A. Imran, H. A.Badran, H. S. Shaker, A. Alsalihi and K. I. Ajeel, J. of Materials Science: Materials in Electronics, **30**,10284 (2019).
16. R. K. Fakher Alfahed, H. A. Badran, F. Zuhair Razzooqi and K. K Mohammad, IOP Conf. Series: Materials Science and Engineering 928, 072071 (2020).
17. H.A. Badran, Appl. Phys. B **119**, 319 (2015). https://doi.org/10.1007/s00340-015-6068-2
18. H.A. Badran, Adv. Phys. Theor. Appl. **26,** 36(2013).
19. M. T. Obeed, R. CH. AbuL-Hail and H. A. Badran, Journal of Basrah Researches (Sciences), **46**(1), 49 (2020).
20. H. A. Bdran, R. C. H. Abul-hail and M. T. Obeed, AIP Conference Proceedings **2290,** 050035 (2020).
21. R. K. Fakher Alfahed, K. K. Mohammad, M. S. Majeed, H. Ali Badran, Kamal M. Ali, B and Yahya Kadem, IOP Conf.
Series:Journal of Physics: Conf.Series**1279**, 012019 (2019).
22. R.K. Fakher Al-fahed, A. Imran, M.S. Majeed and H. A. Badran, Phys. Scr. **95**, 075709 (8pp) (2020).
https ://doi.org/10.1088/1402-4896/ ab7e3 3
23. H. A. Badran, A. A. Al-Fregi, R. K. Fakher Alfahed and A.S. Al-Asadi, of Materials Science: Materials in Electronics,
28,17288 (2017).
24. H. A. Badran, K. A. Al-Adil, H.G. Lazim and A.Y. Al-Ahmad, of Materials Science: Materials in Electronics **27**, 2212 (2016).
25. R. K. Fakher Alfahed, A. Imran, H. A. Badran and A. Al-Salihi, J. of Materials Science: Materials in Electronics. **31**, 13862(2020).
26. H. A. Badran, A. Y. AL-Ahmad, M. F. AL-Mudhaffer and C. A. Emshary Opt. Quant. Electron.**47**,1859 (2015).
27. H. A. Badran, A.Y. Taha, A.F. Abdulkader and C.A. Emshary, J. Ovonic Res. **8,** 161 (2012).
28. A.Y. AL-Ahmad, M. F. AL-Mudhaffer, H.A. Badran and C.A. Emshary, Opt. Laser Technol. **54**, 72 (2013).
29. F.A. Al-Saymari, H.A. Badran, A.Y. Al-Ahmad and C.A. Emshary, Indian J. Phys. **87,**1153 (2013).
30. A. A. Hussain, A. A. Musa, R. K. Fakher Alfahed and H. A. Badran, AIP Conference Proceedings **2290**,050049 (2020).
31. H. A. Badran, Results Phys. **4**, 69 (2014).
32. H. A.Al-Hazam, R. K.Fakher Al-fahed, A. Imran, H. A.Badran, H. S.Shaker, A.Alsalihi and K. I. Ajeel, J. of Materials Science: Materials in Electronics, **30** (11),10284 (2019). https://doi.org/10.1007/s10854-019-01365-2
33. K. Abd AL-Adel and H. A. Badran, European Journal of Applied Engineering and Scientific Research,**1**(2), 66 (2012).
34. K. Abd AL-Adel and H. A. Badran, Journal of Basrah Researches (Sciences) **38**(4) A, 73 (2012).
35. B. Kadem, R. K. Fakher Al-fahed, A.S. Al-Asadi and H. A. Badran, Optik **204**, 164153 (2020).
36. R. K. Fakher Al-fahed, A. S. Al-Asadi, M. F. Al-Mudhaffer and H. A. Badran, Optics and Laser Technology **133**,106524 (2021).
37. H. A. Badran and H. A. Hasan, AIP Conference Proceedings **2290**, 050037 (2020).
38. A. Hohmuth and W. Weissflog, Liq. Cryst. **22**(2) 107 (1997).
39. G.W. Gray, Ther-motropic Liquid Crystals, John Wiley, Chichester and New York, 1987.
40. B.Y. Zhang, F.B. Meng, M. Tian and W. Q. Xiao, React. Funct. Polymer, **66,** 551(2005).
DOI: 10.1016/j.reactfunctpolym.2005.10.030
41. F.Yuksel, D. Atilla and V. Ahsen, Polyhedron, **26,** 4551 (2007).
42. B. E. Eran, A. Nesrullajev and N.Y. Canli, Mat. Chem. Phys. **111**, 555 (2008).
43. S.T. Ha, L.K. Ong, S.T. Ong, G.Y. Yeap, J.P.W Wong, T. M. Koh and H.C. Lin, Chin. Chem. Lett. **20**, 767 (2009).
44. A .K. Prajapati and C.C. Varia, Liq. Cryst. **35**, 1271(2008).

45. G.Y. Yeap, S.T. Ha, P.L. Boey, W.A.K. Mahmood, M. M. Ito and Y. Youhei, Mol. Cryst. Liq. Cryst. **452**,73 (2006).
46. G.Y. Yeap, S.T. Ha., P.L. Boey, M.M. Ito, S. Sanehisa and Y. Youhei, Liq. Cryst. **33**, 205 (2006).
47. Z. Belarbi, G. Guillaud, M. Maitrot, J. Huck, J. Simon and F. Tournilhac, Revue de Physique Appliquee, **23**,143 (1988).
48. W. J. Mc Carter, G. Starrs, T. M. Chrisp, P. A. M. Basheer and S. V. Nanukuttan, Journal of Materials Science **7**,56 (2015). DOI: 10.1007/s10853-014-8669-2.
49. S. K. Prasad, K. L. Sandhya, G. G. Nair, U. S. Hiremath C.V. Yelamaggad and S. Sampath, Liquid Crystals **5**,120 (2006).
50. Salam Hussein Ewaid et al 2020 J. Phys.: Conf. Ser. 1664 012143.
51. Salam Hussein Ewaid et al 2021 IOP Conf. Ser.: Earth Environ. Sci. 722 012008
52. P. Tripathi, S. Dixit and R. Manohar, Chemical Rapid Communications, **1**(2),50 (2013).
53. Salam Hussein Ewaid et al 2021 IOP Conf. Ser.: Earth Environ. Sci. 790 012075.
54. Ahmed Alaa Kandoh et al 2021 IOP Conf. Ser.: Earth Environ. Sci. 790 012073.
54. M. Frasa, M. Marzeca, S. Wrobel, M. D. Ossowska Chrusciel and J. Chrusciel , Acta Physica Polonica A **113**,1155 (2008).